ELSEVIER

Dyes and Pigments 46 (2000) 69–79

DYES and PIGMENTS

Analysis of regulatory dye in diesel petroleum

Russell Timkovich

Department of Chemistry, University of Alabama, Tuscaloosa, AL 35487-0336, USA

Received 23 June 1999; accepted 29 February 2000

Abstract

This study is concerned with alternative analytical methods for determining the content of red dye in diesel fuel. It was found that a preconcentration step consisting of adsorption chromatography on silica gel, followed by either HPLC or gas chromatography–mass spectrometry greatly increases the sensitivity of the method employed. Structures for the main components in the commercial dye are proposed based on NMR data. © 2000 Elsevier Science Ltd. All rights reserved.

Keywords: Chromatographic analysis; Diesel fuel; Oil Red EGN; Solvent Red 26

1. Introduction

While US motorists are acutely aware that certain taxes are applied to gasoline, they may be unaware of the special regulations associated with diesel fuel. Diesel fuel used in normal vehicle road traffic by automobiles and trucks is subject to taxation, and in the state of Alabama this fuel is taxed at 17 cents/gallon. However, off-road machinery using diesel fuel, such as tractors, boats, farm, and logging equipment, are exempt from the on-road tax [1]. In order to differentiate the two types of fuel, an intense red dye is added to the tax-exempt off-road fuel. Since 1994, federal and state laws have mandated the addition of red dye spectrally equivalent to 11.1 mg C.I. Solvent Red 26 (**1**), also known as Oil Red, per liter of fuel. Mandating the use of an additive in the non-taxed fuel rather than the taxed class prevents illegal use practices. Solvent Red 26 is part of a family of red dyes that have general structure (**2**).

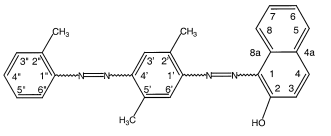

1

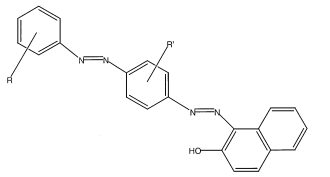

2

Compliance with regulations is relatively easy to check using visible absorption analytical techniques. In this regard, second derivative spectroscopy can be used to compensate for the highly variable sloping absorption baseline arising from the complex natural hydrocarbon matrix. In the early stages of the studies reported here, second derivative spectral intensities of stock solutions of Solvent Red 26 in the range of 7–15 mg/l were measured with a precision of 7%. Dyed diesel fuels supplied by local distributors were also analyzed and found to contain at least the required dye concentration.

The precision and sensitivity of derivative spectroscopy falls when the dye level drops below ca. 2

PII: S0143-7208(00)00037-1

mg/l. Analysis is further complicated when secondary colorants are added to colored fuel to mask the spectral response of standard red dye. With these points in mind, the purpose of the present research was to explore practical alternatives to optical detection of red dyes. While the problem appears to be simple in principle, complications arise from the presence of the natural hydrocarbon matrix (fuel) and the chemical heterogeneity of the dye employed.

2. Experimental section

Samples of diesel fuel with and without dye were obtained from petroleum distributors. A 25 g sample of Solvent Red 26 (lot No. EQ11818JN) was obtained from Aldrich Chemical Company. Disposable solid-phase extraction columns packed with silica gel (Baker 10SPE No. 7086) were obtained from J.T. Baker Research Products. Bulk chromatographic grade silica gel of the same porosity (40 μm with 60-Å pore diameter) was obtained from Spectrum Chemical Company. Merck silica TLC plates were obtained from Alltech Associates, Inc., and solvents were ACS Reagent grade from Fisher Scientific.

Preconcentration silica gel columns were washed with 5 column volumes of neat chloroform, then equilibrated by washing with 15 column volumes of hexane. Dye fractions were dried on a rotary evaporator or under a stream of dry nitrogen gas.

Visible spectroscopy was performed on a Perkin-Elmer Lambda 5 double-beam spectrophotometer. Derivative spectroscopy was performed according to standard methods [2] in 1-cm cuvettes. First derivative spectra were scanned at 15 nm/min with an instrument response factor of 1 s, using a 2-nm slit width and $\Delta\lambda$ of 2 nm. The λ_{max} for the band of an absorbing species was determined as the zero-crossing point of the first derivative spectrum. Second derivative spectra were scanned at 5 nm/min with a response factor of 10, using a 4 nm slit width and $\Delta\lambda$ of 4 nm.

HPLC was performed on 5 μm Whatman Partsil silica gel columns (250 × 4.6 mm) eluted at 1 ml/min using a Perkin-Elmer LC95 UV–visible detector set at 519 nm. Peaks were quantified using a Thermo-Separations Model SP4290 Computing Integrator. Dye samples from diesel fuel were preconcentrated. The same protocol was used to remove dark brown impurities from the dye from Aldrich Chemicals in order to prevent premature degradation of the analytical HPLC columns. Samples used in NMR analyses were obtained by pooling fractions from repetitive injections. In some cases, the combined fractions were re-chromatographed using re-distilled solvents, to remove trace impurities and to improve resolution from components having comparable retention times.

^{1}H NMR spectra (500 MHz) were recorded at 295 K in 99.6 + % dichloromethane-d_2 (Aldrich). Chemical shifts are reported nominally against TMS as 0 ppm, but the residual CH_2Cl_2 was used as the actual internal standard (5.320 ppm for ^{1}H, 53.80 ppm for ^{13}C). Scalar coupling was measured by conventional irradiation techniques or by using 2-D scalar correlation magnitude mode COSY experiments [3].

Electron impact (EI) mass spectrometry was performed on a triple sector VG AutoSpec instrument. Isolated HPLC fractions were introduced via a heated solids probe with heating at 25–200°C. Exact mass measurements were performed with perfluorokerosene as the internal standard. Gas chromatography (model HP5890GC) used He carrier gas with a column volume flow of 3.7 ml/min in a short 3 m capillary column (0.25 mm I.D.) of OV-1 (dimethylpolysiloxane, from Alltech Associates). $CHCl_3$ solutions of preconcentrated dye (typically 1.5–5 μg total dye/μl) were diluted with acetone to achieve injection concentrations of 0.5 ng/μl–1.5 μg/μl. Samples (1 μl) were injected splitless through a deactivated glass liner with the purge off. The temperature program consisted of an isothermal 160°C step for 0.5 min followed by heating to 300°C at 45°C/min and holding at 300°C until the chromatography was complete. Mass spectral acquisition was gated off to allow the solvent peak to clear. Scanning GC–MS experiments were conducted over the 500–50 mass range, at 1 scan/s, and single ion monitoring experiments were conducted at a resolution of 1000. Single ion response was monitored continuously, or the instrument was programmed to sample a

reference compound lock mass to insure long term stability. Since the chromatograms were relatively short, no differences were noted in the results from the two methods. Given that the preconcentrated dye samples from diesel fuel contained a substantial hydrocarbon background, the GC column requires cleaning and reconditioning, or replacing when the dye peak broadens. This occurs after 3–4 injections of >500 ng total dye/injection, but the frequency decreases linearly as the concentration per injection decreases.

The main focus of the present study was to assess different methods for the analysis of red dye in diesel fuel.

3. Results and discussion

3.1. Sample preparation

Direct analysis of dye in diesel fuels by non-optical spectroscopic methods was very difficult because of the extensive hydrocarbon background. Preconcentration of colored fuel prior to analyses, by evaporation or distillation of the fuel, was not practical because of the high boiling point of various diesel fuel components. Fortunately, the hydroxyl group, azo groups, and the extended aromatic systems of structure **2** led to strong adsorption of the dye on silica gel. To effect separations, colored fuel samples were applied to chromatographic-grade silica gel that had been equilibrated with hexane, and flash chromatography was conducted using a column head pressure of 4–5 psi with N_2. Red dye bound tightly to the column which was then washed with 20 column volumes of hexane. The hexane wash eluted viscous yellow material that had a low affinity for the silica. The column was then eluted with 1:1 hexane:$CHCl_3$ and the red dye eluted as a broad band that was easily monitored visually and collected. Four column volumes of hexane:$CHCl_3$ was sufficient to elute all the red dye. Following preconcentration of dilute dye samples, collection of the column effluent began when the solvent-change front, which was very evident due to the refractive index change in going from hexane to the chloroform blend, reached the column bottom. The dye effluent afforded an oily residue following concentration, and the isolated dye was redissolved in $CHCl_3$ as a concentrated stock solution.

At this stage, optical spectroscopy was applied to the more concentrated dye solution and the results were used to determine the original dye concentrations in fuel samples. For example, a sample of 1 part standard colored fuel (11.1 μg/ml) was diluted with 99 parts uncolored fuel and preconcentrated by passing 50 ml of solution through a silica gel column. Optical analysis readily afforded the correct diluted concentration. This chromatographic step was very useful in clearing the natural absorption background of fuel samples, as dark material remained bound to the adsorbent.

The efficiency of the preconcentration step was not limited by the amount of dye present, but instead by the extent to which (a) fuel competed with the dye for silica adsorption sites and (b) fuel constituents acted as eluents for the dye. The practical limitation was the fuel to silica ratio and this ratio may be variable because of the differences in available petroleum stocks. In the present study, the maximum ratio was 10 ml fuel per 1 cm^3 (0.5 g) settled volume of 200 mesh dry silica gel. Colored diesel fuel that was concentrated under such conditions was still impure, as evident from the oily nature of the eluted dye. NMR and mass spectral analyses of the resultant dye showed a complicated hydrocarbon background from which it was not possible to identify the dye.

While preconcentration was designed to improve the results of optical analysis, it also facilitated the evaluation of other analytical methods. In this regard, TLC was investigated but was judged to be unsatisfactory for quantification. It was found that preconcentrated dye from fuel afforded a comet-shaped chromatogram with multiple components, due to residual hydrocarbons and the chemical heterogeneity of the commercial dye.

3.2. HPLC optimization

Following the solvent selectivity guidelines of Kirkland and Snyder [4] the following binary mixtures were considered: chloroform (30 parts by volume):hexane (70 parts); benzene (50):pentane (50); toluene (50):pentane (50); dichloroethane (25):

hexane (75); methyl, *t*-butyl-ether (2.5):hexane (97.5); isopropyl ether (5):hexane (95); dichloromethane (15): carbon tetrachloride (85); ethyl acetate (1.5): hexane (98.5): 2-butanone (1.5):hexane (98.5); dioxane (2.5):hexane (97.5); 1-chlorobutane (50):pentane (50); 2-bromopropane (60):pentane (40). Although the chromatograms obtained were quite similar, there were subtle differences in the resolution of individual components. With the principal aim of maximizing the separation of component Al9 from Al8, chloroform–hexane, toluene–pentane, and dichloromethane–carbon tetrachloride were found to be the preferred systems, giving chromatograms such as the one shown in Fig. 1. For eight replications involving the dye obtained from Aldrich, the relative standard deviation in area for a large peak in which there is partial overlap with an adjacent peak (cf. Al8 with Al9) was 4.6%. For resolved peaks like Al7 and Al12, the relative standard deviation was 2.3–3.6%. The integrated areas were verified to be linear with concentration from 100 μg total dye injected to the lower limit of detection [5] of 10 ng total dye injected. Since 46.5% of total dye was Al8 (see Table 1 for other relative amounts), this gave a lower limit for a single component of around 5 ng. Above 100 μg per injection, there was significant peak broadening and loss of resolution, indicating column overload. For diesel fuel samples, a limiting factor was the volume of oily residue (~1–2 μl per ml of original diesel fuel) remaining after the pre-concentration step. The resultant liquid was too viscous for direct injection and required diluting with at least an equal volume of solvent. Assuming a maximum of 2 μl of oily residue per ml of starting fuel, the sample must be diluted 1:1 with a non-viscous solvent such as hexane or chloroform before injection, giving 4 μl of injectable sample per ml of original fuel.

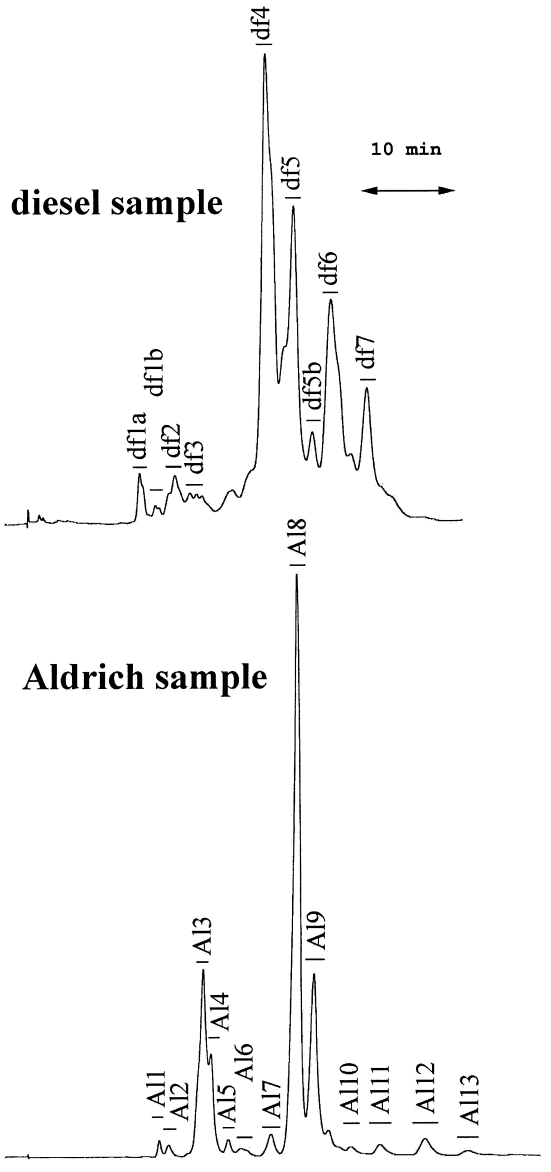

Fig. 1. HPLC chromatograms of a pre-concentrated dye sample from diesel fuel and Solvent Red 26 from Aldrich, following a 40 μg total dye injection, with the detector set at 1 absorbance unit full scale and 519 nm, and eluting with chloroform:hexane (3:7) at 1 ml/min.

The analytical HPLC columns employed injector loops in the range of 10–100 μl. The high limit meant that final residue from a maximum of 25 ml of original fuel was the most that could be injected. If this residue after preconcentration contained at least 5 ng of a single component, then it would be detected. At 5 ng/25 ml or 0.2 ng/ml, compared to the regulatory level of 11.1 μg/ml, this means that a dilution of 55,000-fold would be detectable.

By taking advantage of the aforementioned detection levels, HPLC analysis of pre-concentrated diesel fuel samples could be employed as a more sensitive technique than optical spectroscopy for detecting and quantifying red dye content.

However, it was necessary to specify precisely the component(s) to be analyzed. One could specify the major component, a set comprising the most abundant components, or the complete set of red components. The complete-set option would be difficult to achieve when using dilute dye samples because the minor components can not be accurately measured. Fixed wavelength detection was employed in the present study; specificity would be enhanced by using rapid scanning or photodiode array detectors.

Table 1
Summary of spectroscopic data for dye components

Fraction[a]	Assigned structure	λ_{max}[b] (nm)	%df[c]	%Al[d]	m/z[e]	NMR spin subsystems[f] {multiplicity(ppm)–multiplicity(ppm)}
Al1 = df1a	n.a.[g]	489	4.2	0.6	n.d.[h]	n.d.
Al2 = df1b	n.a.	519	1.4	0.8	n.d.	n.d.
Al3	**7**	524		13.2	394	{d(7.755)–d(6.827)} {d(8.628)–t(7.590)–t(7.443)–d(7.627)} {s(8.085)} {s(7.636)} {d(7.648)–t(7.287)–t(7.279)–d(7.371)} methyls (2.833, 2.763, 2.551)
Al4 = df3	**8**	526	4.0	6.1	408	{d(7.756)–d(6.834)} {d(8.632)–t(7.601)–t(7.441)–d(7.630)} {s(8.074)} {s(7.619)} {d(7.610)–d(7.087);s(7.190) methyls (2.818, 2.731, 2.549, 2.390)
Al5		519		1.3	394	n.d.
Al6		519		1.4	408	n.d.
Al7 = df4	**14** or **15**	518	32.6	2.0	394	{d(7.763)–d(6.834)} {d(8.598)–t(7.591)–t(7.441)–d(7.626)} {d(8.248)–d(7.959);ps(7.890)} {d(7.671)–t(7.295)–mult(7.41)[2H]} methyl (2.635) {ethyl q(3.202)–t(1.328)}
Al8 = df5	**3**	518	16.3	46.5	380	{d(7.763)-d(6.837)} {d(8.596)–t(7.593)–t(7.444)–d(7.628)} {d(8.248)–d(7.965);ps(7.897)} {d(7.656)–t(7.294)–t(7.277)–d(7.382)} methyls (2.753, 2.631)
Al9 = df5b	**4**	519	4.3	17.3	394	{d(7.762)–d(6.839)} {d(8.600)–t(7.588)–t(7.438)–d(7.627)} {d(8.233)–d(7.936);ps(7.868)} {d(7.595)–d(7.092);ps(7.194)} methyls (2.721, 2.626, 2.391)
Al10 = df6	**6**	518		1.5	408	{d(7.769)–d(6.883)} {d(8.425)–t(7.572)–t(7.423)–d(7.587)} {s(7.759, [2H])} {d(7.653)–d(7.092);ps(7.196)} methyls (2.747[6H], 2.726, 2.393)
Al11 = df7	**12**	519	15.1	1.9	394	{d(7.761)–d(6.833)} {d(8.600)–t(7.591)–t(7.440)–d(7.625)} {d(8.241)–d(7.943);ps(7.885)} {d(7.863[2H])–d(7.378[2H])} methyl (2.624) {ethyl q(2.750)–t(1.294)}
Al12	**5**	519	8.0	2.6	394	{d(7.761)–d(6.834)} {d(8.600)–t(7.590)–t(7.439)–d(7.626)} {d(8.237)–d(7.932);ps(7.872)} {d(7.302)-d(7.678);ps(7.732)} methyls (2.622, 2.381, 2.358)
Al13	**13**	526		1.4	408	{d(7.755)–d(6.829)} {d(8.627)–t(7.604)–t(7.442)–d(7.627)} {s(8.077)} {s(7.649)} {d(7.864[2H])–d(7.370[2H])} methyls (2.814, 2.544) {ethyl q(2.748)–t(1.293)}

[a] Fractions isolated by HPLC corresponding to the peaks labelled in Fig. 1.
[b] Determined by first derivative visible spectroscopy.
[c] Determined by integration of the diesel fuel HPLC chromatograms.
[d] Determined by integration of the HPLC chromatograms of the Aldrich research dye sample.
[e] Observed molecular parent ion in mass spectrometry.
[f] {}d = doublet, t = triplet, s = singlet, and ps = pseudo-singlet.
[g] n.a., not assigned.
[h] n.d., not determined.

Following separations, visible absorption, mass spectrometric, and NMR analysis of the isolated constituents were used establish the structures of each dye component.

3.3. Absorption and mass spectral analyses

The visible spectra of the isolated components were nearly identical, with each showing a broad band near 520 nm. However, when first derivative spectroscopy [2] was employed, it was clear that two types of colorants were present, one with λ_{max} in the range 517–519 nm, and the other with λ_{max} in the range 522–526 nm. These results are consistent with the presence of constituents arising from the use of isomeric substituted anilines in the synthesis of the commercial dye.

Mass spectrometry of the isolated components revealed that a major difference among them was the number and distribution of methyl groups.

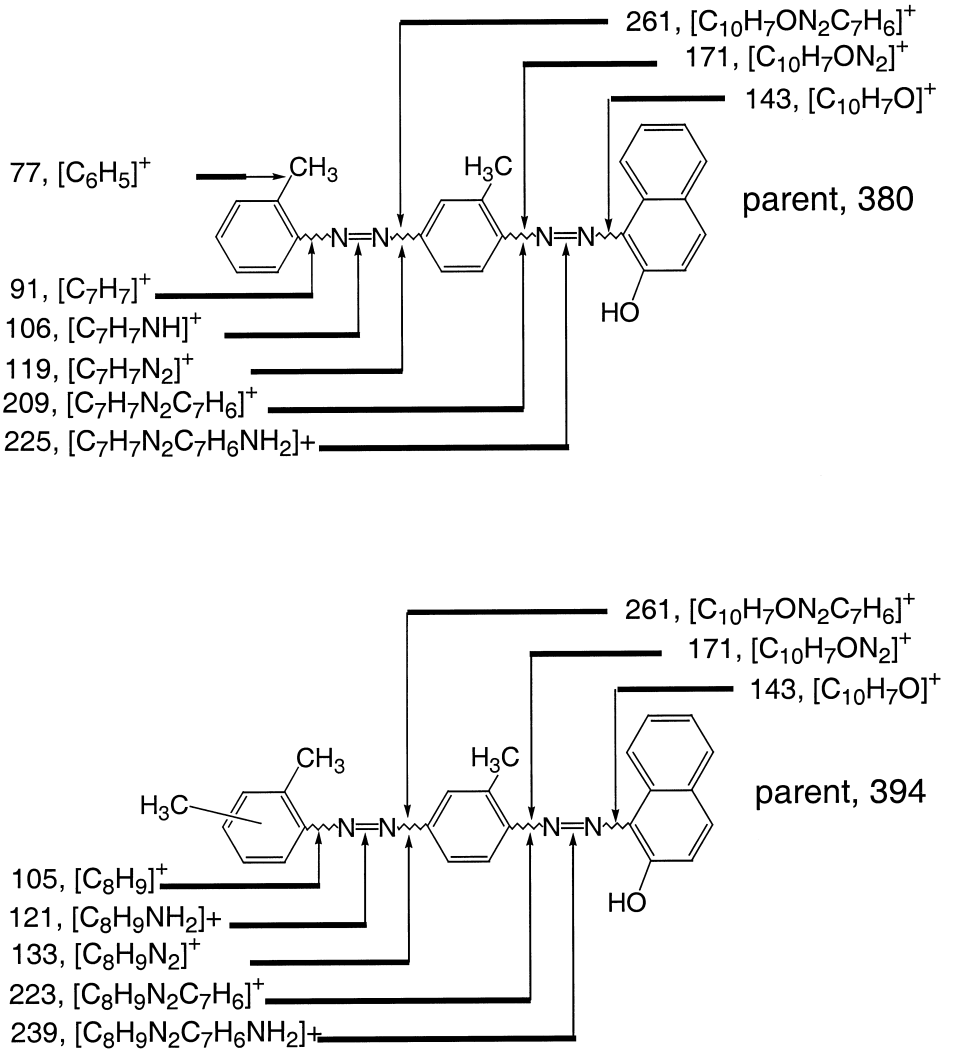

Fig. 2. Summary of fragment ions observed in the electron impact mass spectra (70 eV) of fractions isolated with parent ions of m/z 380 or 394.

The components showed a parent molecular ion of either m/z 380 [typical obs. mass 380.163 ($\sigma = 2.6$ mDa); calc. 380.1637 for $C_{24}H_{20}N_4O$, nominal two methyls], 394 [typical obs. mass 394.179 ($\sigma = 1.6$ mDa); calc. 394.1794 for $C_{25}H_{22}N_4O$, nominal three methyls], or 408 [typical obs. mass 408.194 ($\sigma = 1.7$ mDa); calc. 408.1950 for $C_{26}H_{24}N_4O$, nominal four methyls]. The mass spectral fragmentation pattern (summarized schematically in Fig. 2) was also informative. As anticipated, the major fragments corresponded to breaking the carbon-nitrogen bonds that are adjacent to the azo group. Ions were also observed for fragments arising from reductive-cleavage of the azo bond via NH–NH bond scission. The fragmentation pattern also indicated that the middle phenyl ring was mono-methyl substituted in the component having m/z 380 and in many of the components having m/z 394, contrary to the expected structure **1** for Solvent Red 26.

HPLC fractions from colored diesel fuel were too contaminated with hydrocarbons to yield useful NMR spectra of the dye components. However, fractions isolated from the Aldrich dye were free from non-dye contaminants and afforded interpretable NMR spectra.

3.4. NMR spectra

NMR data are summarized in Table 1, including the wavelength maximum observed in absorption spectra, the relative amounts of each component in both the fuel and Aldrich dye samples, the observed molecular ion, and observed ^1H chemical shifts. NMR chemical shifts are arranged according to the coupling patterns observed and reported according to the following scheme. Brackets {} enclose mutually coupled spin subsystems; apparent first order multiplicity of the peak is indicated as d for doublet, t for triplet, s for singlet and ps for pseudo-singlet with the observed chemical shift reported in parentheses in ppm, (ppm). For example, the second line for fraction Al7 is {d(8.598)–t(7.591)–t(7.441)–d(7.626)}. This means there was a doublet at 8.598 ppm coupled to a triplet at 7.591 ppm that was coupled to another triplet at 7.441 ppm that was coupled to a doublet at 7.626 ppm. Placing these resonances within the brackets means they were not coupled to any other resonances in the spectrum. For reasons to be discussed, the first two subsystems have been assigned to the naphthol ring. The third subsystem has been assigned to the middle phenyl ring and the last subsystem has been to the terminal phenyl ring as depicted in structure **1**. The coupling observed within spin subsystems was typical vicinal coupling of 7.6–8.2 Hz, except for the first subsystem which showed 9.5 Hz coupling. The "ps" resonances were pseudo-singlets that showed long range W-coupling of 1–1.8 Hz to the "d" resonances preceeding them. Aromatic resonances integrated to one proton and methyls to three protons except in a few cases of degenerate resonances which are marked as [nH] where n represents the relative area in units of protons. In subsequent discussion the ring numbering scheme of structure **1** will be used and protons are designated according to the attached carbon, i.e. H(C3) is the proton at ring position 3.

The main component (Al8; m/z 380) had methyl resonances at 2.753 and 2.631 ppm. Aromatic protons included coupled doublets at 7.763 and 6.837 that had a coupling constant of 9.5 Hz. These signals were assigned to H(C4) and H(C3), respectively, on the naphthol moiety because these ring positions show large vicinal coupling constants in other polyaromatic hydrocarbons [6]. The upfield proton was confirmed to be H(C3) in the ^{13}C studies discussed below. A vicinally coupled spin subsystem composed of a doublet (8.596 ppm), triplet (7.593 ppm), triplet (7.444 ppm), and doublet (7.628 ppm) arose from the four adjacent protons H(C5)–H(C8). These six proton resonances were present in the NMR spectra of each component (see Table 1). This indicated that the naphthol unit was not the source of heterogeneity in the Aldrich dye. The proton NMR spectrum of Al8 contained another subsystem comprising a doublet (7.656 ppm), triplet (7.294 ppm), triplet (7.277 ppm), doublet (7.382 ppm) that was shown to be on the same ring as the methyl group at 2.753 ppm. This assignment resulted from a nuclear Overhauser enhancement (NOE) experiment involving the signals at 2.753 and 7.382 ppm. The signals in this second subsystem were assigned to the terminal

phenyl ring. The remaining signals in the spectrum consisted of the 2.631 ppm methyl that showed an NOE to a "pseudo-singlet"; at 7.897 ppm. This pseudo-singlet showed a long-range W-coupling of 1.4 Hz to the doublet at 7.695 ppm, which in turn showed vicinal coupling to the doublet at 8.248 ppm. These observations were consistent with a mono-methylated middle phenyl ring.

The ^{13}C spectrum of Al8 was assigned (Table 2) by the 2-D proton–carbon correlation techniques HMQC [7] and HMBC [8]. Values obtained for the naphthol carbons are in agreement with a previous report for 1-phenylazo-2-naphthol [9], except that the present study suggests interchanging the C4 and C5 assignments, which were problematic in the earlier study. C1′ was assigned to the 144.41 ppm resonance on the basis of chemical shift homology to the model compound 1-phenylazo-2-naphthol, and then the remaining assignments follow from the multiple bond correlations of the HMBC experiment. The ^{1}H and ^{13}C assignments indicate structure **3** for the Al8 component.

The next most abundant component Al9 gave the same proton spin subsystems for the middle and naphthol rings as observed for Al8. Its parent ion of 394 indicated a third methyl group and a new methyl resonance was observed at 2.391 ppm. This methyl group gave an NOE to a pseudo-singlet at 7.194 ppm that showed long range W-coupling (1 Hz) to the doublet at 7.092 ppm, which in turn showed vicinal coupling to the doublet at 7.595 ppm. The new doublets were assigned to H(C4″) and H(C5″) by chemical shift homology to the corresponding protons in Al8. This pattern establishes the structure as **4**.

Component Al12 (*m*/*z* 394, three methyls) gave the same proton NMR spin subsystems as the middle and naphthol rings of Al8. The spectrum was missing the 2.75 ppm methyl common to Al8 and Al9, but showed a methyl resonance at 2.381 ppm that was assigned to CH_3(C6″) based upon homology to Al9, and a new methyl resonance at 2.358 ppm. The spectrum contained a new subsystem consisting of a pseudo-singlet W-coupled to the doublet at 7.678 ppm, which in turn was vicinally coupled to the doublet at 7.302 ppm. By chemical shift homology to Al8, the latter doublet was assigned to H(C2″) and the structure assigned was **5**.

The proton NMR spectrum of component Al3 had homologous resonances to the naphthol group and the terminal phenyl ring of Al8. Rather than showing the resonances of the middle ring of Al8, the spectrum had singlets at 8.085 and 7.636 ppm and methyl resonances at 2.833 and 2.551 ppm. Component Al4 afforded the expected naphthol group resonances, the subsystem for the terminal ring of Al9, and the same middle ring subsystem as Al3. The spectrum of component Al10 was also homologous to Al9 in terms of the naphthol and terminal rings, but had unique resonances at 7.759 ppm (singlet) which integrated for two protons, and a resonance at 2.747 ppm (methyl) which integrated for six protons. Components Al3 and Al4 with respect to Al10 are

Table 2
^{13}C assignments for component Al8

	Carbon[a]	^{13}C shift[b] (ppm)
1	C1(N=N)	131.90
2	C2(OH)	176.16
3	C3(H)	125.99
4	C4(H)	141.66
5	C5(H)	129.24
6	C6(H)	126.77
7	C7(H)	129.57
8	C8(H)	122.26
9	C4a(C)	128.69
10	C8a(C)	133.83
11	C1′(N=N)	144.21
12	C2′(H)	129.05
13	C3′(CH_3)	126.05
14	C4′(N=N)	151.23
15	C5′(H)	122.96
16	C6′(H)	116.31
17	CH_3(C3′)	17.67
18	C1″(N=N)	151.23
19	C2″(H)	131.68
20	C3″(CH_3)	138.73
21	C4″(H)	115.58
22	C5″(H)	126.78
23	C6″(H)	131.29
24	CH_3(C3″)	17.83

[a] In parentheses is given the group attached to this carbon, to differentiate proton-bonded from non-proton-bonded carbons.

[b] In deuterated dichloromethane at 296 K referenced against the dichloromethane carbon at 53.80 ppm.

related in having two singlets and two methyl groups attached to the middle ring, and there are only two ways to position substituents to achieve this coupling arrangement. Because of the chemical shift degeneracy, Al10 was assigned structure **6** which has an approximate 2-fold symmetry axis perpendicular to the middle ring. Component Al3 was accordingly assigned structure **7** and Al4 was assigned structure **8**, where the middle ring does not have the approximate 2-fold symmetry axis.

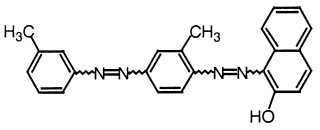

3

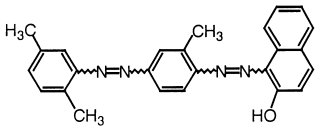

4

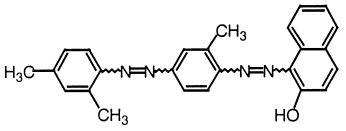

5

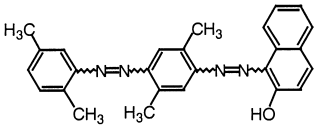

6

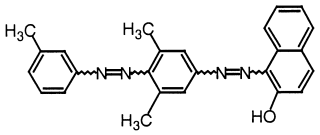

7

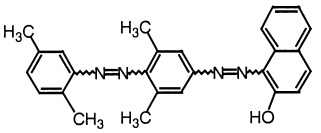

8

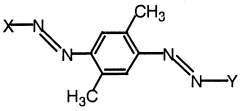

9

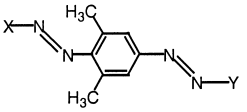

10

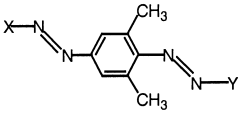

11

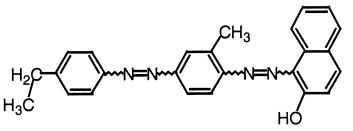

12

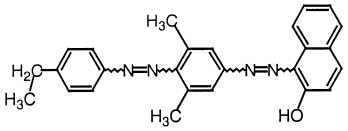

13

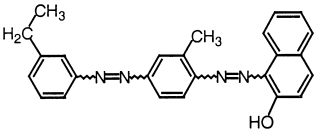

14

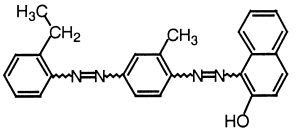

15

The approximate symmetry axis is more evident in structures **9** and **10** where the (*E*)-configuration is explicitly shown. It is possible that the middle ring for Al3 and Al4 should be reversed as shown for **11**.

The proton NMR spectrum of component Al11 had the same middle ring and naphthol resonances as Al8. Interestingly, rather than showing the expected methyl resonances, an ethyl spin system (triplet at 1.294 ppm and quartet at 2.750 ppm) was observed. These observations, along with two coupled doublets at 7.863 and 7.378 ppm, led to the assignment of **12** as the structure. Component Al13 gave the same terminal ring resonances as Al11 and the same middle ring resonances as Al3 and Al4 and was assigned structure **13**.

The proton NMR spectrum of component Al7 (cf. also df4, the main component in the diesel samples) contained the same resonances for the naphthol and middle rings as Al8, and like Al11 and Al13 revealed an ethyl group. The remaining aromatic resonances were a doublet a 7.671 ppm coupled to a triplet at 7.295 ppm. The latter was coupled to a complex multiplet at 7.4 ppm that integrated for two protons and that overlapped H(C6). The overlap precluded assignment of the protons associated with the multiplet. It is apparent that these signals arose from second-order coupling. If the multiplet were a first-order doublet and a singlet, the structure must be **14**. If it were a first-order triplet and a doublet, the structure must be **15**.

Structures could not be proposed for the remaining minor components due to insufficient sample, impurities, poor resolution from other components, or significant signal overlaps.

Tentative identification of the dye components in commercial diesel fuel was achieved by comparing the absorption spectra and HPLC retention

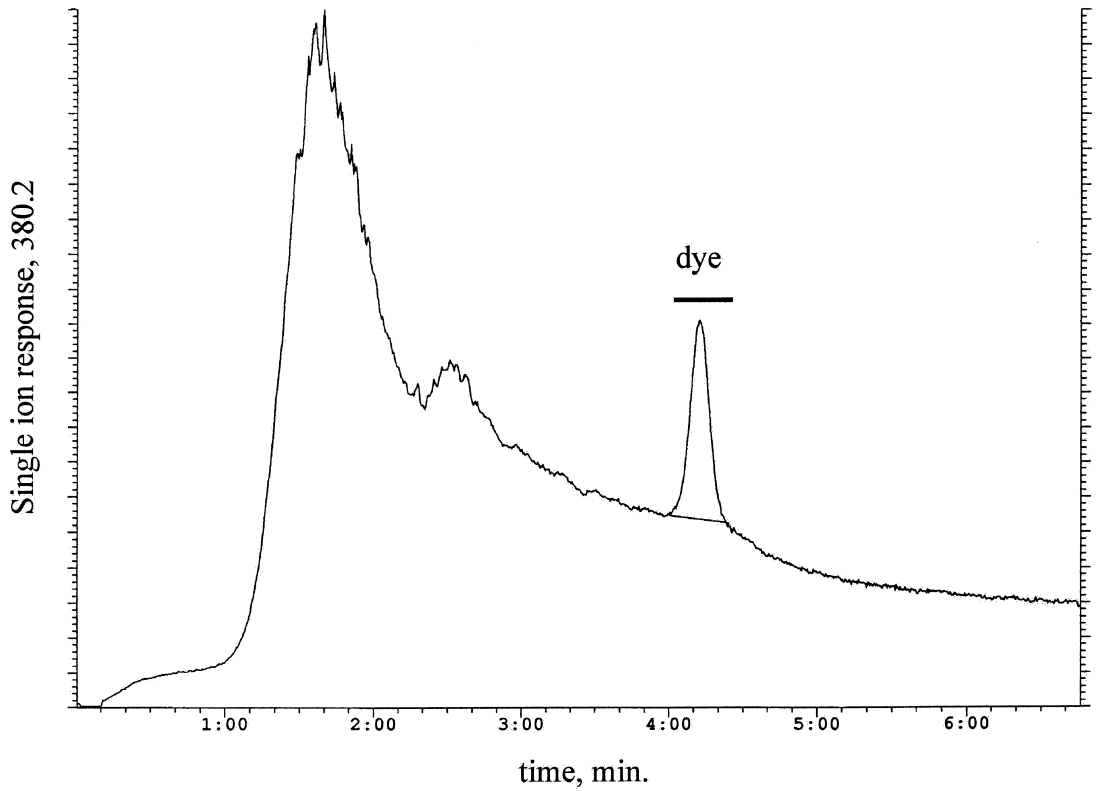

Fig. 3. Single ion response GC–MS chromatogram at *m*/*z* 380.2 of a pre-concentrated dye sample (40 ng total dye) from diesel fuel.

times with the data generated using the Aldrich dye. None of the major dye components in the diesel fuel samples corresponded to the structure expected for Solvent Red 26. The major components in the fuel samples in the present study were **3**, **14**, and **15**, with the ethylated component (**14/15**) predominant.

3.5. GC–MS analyses

Gas chromatography–mass spectrometry (GC–MS) was examined as a method for detecting Solvent Red 26 in diesel fuel. Direct injection of fuel samples was impossible because of the enormous hydrocarbon background, making preconcentration essential. In this case, analysis was further complicated by the low volatility of the dye. Short columns and high temperatures were required to separate the dye components in a reasonable time, and under these the conditions the chromatographic peaks were relatively broad. Fortunately, the sensitivity of MS is very high, and low levels of dye were detectable.

Mass scanning the GC effluent to detect dye proved unsatisfactory because of the hydrocarbon background in preconcentrated samples. Some success was achieved using the technique of single ion monitoring, in which the mass spectrometer functions as a highly selective mass filter/detector. The experiment is illustrated in Fig. 3 in which the mass spectrometer was set to monitor the parent ion (e.g. m/z 380) of one of the dye components. Detectability of a small amount (40 ng) of total dye was possible, despite the significant hydrocarbon background. However, fluctuations in the background can limit dye detection. For colored diesel fuel samples the lower limit of detection was 4 ng/injection. While the hydrocarbon background can be reduced by monitoring at higher resolution, this also decreases the observable ion current. In addition, the background would not be fully eliminated because the dye does not contain any elements that would lead to a unique mass deficiency or excess versus the hydrocarbon fuel itself.

Fig. 3 illustrates that gas chromatography did not resolve all the individual components. However, single ion monitoring at m/z 394 afforded chromatographic peaks at 4:20 and 4:50, while monitoring at m/z 408 afforded a single peak at 5:10.

When Aldrich research dye was analyzed there was no hydrocarbon background and the lower limit of detection [5] was 0.5 ng (total dye)/injection.

4. Conclusions

Preconcentration using a silica gel column before the analysis of dye in diesel fuel gives increased sensitivity for dye detection. The limiting factor in dye detection is the remaining hydrocarbon background rather than sample size or inherent spectral sensitivity. HPLC and GC–MS greatly extend the lower limit of dye detection. While it may be possible to improve dye detection by using more sophisticated techniques such as GC–MS–MS, this would also greatly increases the cost level of the analysis. With this is mind, the preferred method would employ HPLC, based upon the combined considerations of column maintenance, analysis time, sensitivity, selectivity, and overall costs.

References

1 US code title 26, section 4082. Code of Alabama 1975, section 40-17-22.
2 Schmitt A. Applied UV spectroscopy: derivative spectroscopy, an introduction with practical examples. Uberlingen (West German): Bodeseewerk Perkin-Elmer & Co., 1977.
3 Derome AE. Modern NMR techniques for chemistry research. Oxford: Pergamon Press, 1987.
4 Snyder LR, Kirkland JJ. Introduction to modern liquid chromatography. New York: Wiley-Interscience, 1979.
5 Committee on Environmental Improvement A.C.S. Guidelines for data acquisition and data quality evaluation in environmental chemistry. Anal Chem 1980:52;2242–49.
6 Jackman LM, Sternhell S. Applicatons of nuclear magnetic resonance spectroscopy in organic chemistry. Oxford: Pergamon Press, 1969.
7 Bax A, Subramanian S. J Magn Reson 1986;67:565–9.
8 Bax A, Summers MF. J Am Chem Soc 1986;108:2093–4.
9 Lycka A, Snobl D, Machacek V, Vecera M. Organ Magn Reson 1981;15:390–3.